Femtosecond Photolysis of Aqueous Formamide

Christian Petersen,[†] Niels Henning Dahl,[†] Svend Knak Jensen,[†] Jens Aage Poulsen,[‡] Jan Thøgersen,[†] and Søren Rud Keiding*,[†]

Department of Chemistry, University of Aarhus, Langelandsgade 140, DK-8000 Aarhus C, Denmark and Department of Chemistry, Göteborg University, SE-412 96 Göteborg, Sweden

Received: November 21, 2007; In Final Form: January 8, 2008

In this work, we investigate the primary photodynamics of aqueous formamide. The formamide was photolyzed using 200 nm femtosecond pulses, and formation of products and their relaxation was followed with ∼300 fs time resolution using probe pulses covering the range from 193 to 700 nm. Following excitation, the majority of formamide molecules (∼80%) converts the electronic excitation energy to vibrational excitation, which effectively is dissipated to the solvent through vibrational relaxation in just a few picoseconds. The vibrational relaxation is observed as a distinct modulation of the electronic absorption spectrum of formamide. The relaxation process is modeled by a simple one-dimensional wavepacket calculation. A smaller fraction of the excited formamide molecules dissociates to the CHO and NH_2 radical pairs, of which 50% escape recombination. In addition to the electronic excitation of formamide, we also observe a small contribution from one-photon ionization of formamide and two-photon ionization and dissociation of the water solvent.

Introduction

In this work we study the fast primary photochemistry of formamide following femtosecond photolysis at 200 nm. Formamide and other simple amides are often studied in an attempt to gain a deeper understanding of the photochemical properties of biological materials because of their structural similarities to the repetitive unit in peptides. For example, the photostability of biological molecules has been intensely studied in order to elucidate the mechanisms by which molecules convert the potentially harmful electronic excitations into vibrational excitations, which subsequently dissipates rapidly to the surrounding water molecules in a matter of a few picoseconds.[1−3]

It is generally accepted that the initial photoexcitation in formamide is mainly of n−π* character,[4−6] moving an electron from a nonbonding orbital near oxygen to an antibonding π orbital near the α carbon and thus shifting the electron density from the oxygen to the carbon atom. However, small quantum yields, short lifetimes, abstraction and isomerization reactions, and low extinction coefficients have prevented a clear picture of the primary photochemistry of simple amides from emerging.[6,7] Using femtosecond transient absorption spectroscopy covering the range from 193 to 700 nm, we observed both the primary photochemical events in aqueous formamide and the strong solvent solute interactions responsible for dissipating the excitation to the solvent.

Few papers have addressed the primary photochemistry of simple aqueous amides since the early work by Volman[8] and later the microsecond flash photolysis studies by Nakashima and Hayon.[9] These groups observed no transient species in the wavelength region from 250 to 700 nm, indicating very little, if any, photochemical activity of the smaller amides. The situation is similar for the gas phase, where relatively few experimental studies of the photolysis and pyrolysis of formamide have been reported.[10] However, numerous studies have been reported on the structural and dynamical properties of ground-state formamide, recently focusing on the dynamics of the amide bond(s) using multidimensional IR spectroscopy.[11] One previous study,[12] central to this work, by Lundell et al. studied the photolysis of formamide immobilized in noble-gas matrices of either Ar or Xe. Lundell et al. used Fourier transform infrared spectroscopy to identify the steady-state photoproducts following photolysis by a 193 nm nanosecond laser pulse. In the Ar matrix the primary product is a weakly bound complex between NH_3 and CO, thought to originate from breaking of the C−N bond in formamide followed by hydrogen-atom transfer from the formyl radical, HCO, to the NH_2 radical. In Xe, intersystem crossing is enhanced, and the HNCO−H_2 complex is observed as the primary product formed through triplet excited states of formamide. However, due to the time resolution of these studies, the primary photochemistry of formamide is not directly observed.

We previously studied the photolysis of both formic acid,[13] the formate ion,[14] acetic acid, and the acetate ion.[15] Common to these studies were the excitation of the weak n−π* transition on the carbonyl group and the subsequent dissociation of the α-carbon bond, C−R (R = OH, O^-). In comparison, the formamide n−π* transition is expected to have more π−π* character due to a solvent-induced blue shift of the n−π* transition and a similar red shift of the π−π* transition.[16] This makes the absorption at 200 nm in formamide much stronger and thus facilitates a detailed study of its primary photochemistry. The previous studies also indicated that the formyl radical in its hydrated form still played a key role in the subsequent recombination dynamics, in spite of the fact that it was unobservable in the transient spectra.[13,17,18] The larger extinction coefficient of formamide thus enables a detailed investigation of the dissociation and recombination dynamics, in particular the solvent-induced vibrational energy relaxation of formamide. The study illustrates the current understanding of the primary

* To whom correspondence should be addressed. Phone +45 8942 3861. Fax +45 8619 6199. E-mail: keiding@chem.au.dk.
[†] University of Aarhus.
[‡] Göteborg University.

10.1021/jp7110764 CCC: $40.75
Published on Web 03/06/2008

photochemical event in small aqueous molecules: The solvent surrounding the reaction site is so efficient in both caging and relaxing the reaction products and transition states that the outcome of the photochemical reaction is largely determined within the first encounter between the photoexcited solute molecule and the solvent. In other words, the solvent, and in particular water, is so efficient in absorbing the excess energy of the reaction that very little energy remains for further reactions after the first few hundredths of femtoseconds.

Experimental Details

The double-beam transient absorption spectrometer utilized in this work is similar to the one used in a previous study.[13,14,19] Briefly, a 1 kHz titanium−sapphire laser system emitting 0.8 mJ, 100 fs pulses at 800 nm is frequency quadrupled to generate 200 nm pulses used to initiate the photolysis. The 200 nm pump has a pulse energy up to ∼12 μJ and pulse duration of approximately 200 fs. The pump pulse is modulated at 0.5 kHz by a mechanical chopper synchronized to the 1 kHz pulse repetition rate and sent through a scanning delay line and a $\lambda/2$ waveplate before it is focused through the sample by a $f = 50$ cm concave mirror. The probe pulses covering the spectral range from 193 to 700 nm are generated by a two-stage optical parametric amplifier (OPA) pumped at 400 nm either directly by doubling the pulses from the OPA or by mixing the OPA pulses with either 800 or 400 nm pulses. The probe beam is then split into a signal and a reference beam. The signal beam is focused onto the sample by an $f = 5$ cm CaF_2 lens and probes the sample inside the much larger area defined by the pump beam. Signal and reference pulses are then detected by matched photodiodes and boxcar integrators before being processed by a digital lock-in amplifier referenced to the 0.5 kHz modulation of the pump pulse.

The sample consists of a <0.1 mm thin liquid jet produced by a homemade nozzle. The flow of formamide through the liquid jet was adjusted to give a fresh sample for every laser pulse. No measurable degradation of the solution was observed during the measurements, but to avoid potential build up of permanent photoproducts the solution was replaced regularly. The reproducibility of the transient absorption data was tested among consecutive scans as well as by repeating the measurements on different days using different samples. The data could be measured on a common absorption scale with an uncertainty of ±10%. The concentration of formamide was 0.1 M, and we used 3 times distilled water. The linear absorption spectrum of formamide is shown in Figure 1. The extinction coefficient of formamide (aq) has its maximum below 190 nm, and at 200 nm the extinction is 820 M^{-1} cm^{-1}. In addition to the main peak, we observe a weak shoulder on the main absorption. This feature, located between 210 and 240 nm, is not dependent on the concentration of formamide, which rules out dimerization as the cause of the weak shoulder. This is in agreement with the observations in ref 20, where the dimer formation prevails above a mole fraction of 0.2 for formamide in water. Calculations of the electronic excitation energies of formamide and eight water molecules, at the CIS(D)/aug-cc-pvdz level, give a strong transition at 180 nm and a weaker one at 213 nm, in good agreement with the observed spectrum.

Results

Figure 2 shows the transient absorption following the 200 nm pump pulse at a few representative probe wavelengths. For a probe wavelength of 193 nm, the experimental data consist initially of a short spike, which we fitted to a Gaussian function.

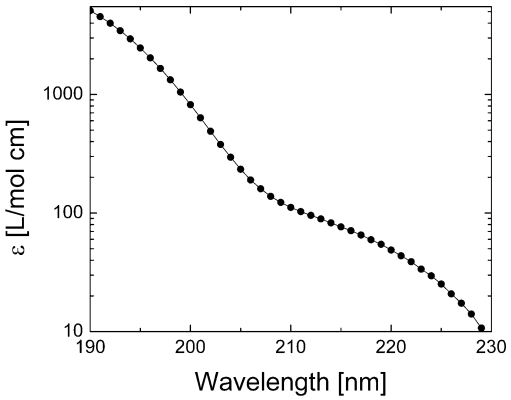

Figure 1. Linear absorption spectrum of formamide (aq). The absorption band peaks below 190 nm and the extinction at 200 nm is 1000 M^{-1} cm^{-1}. On the logarithmic scale a weak absorption band extending from 210 to 240 nm is also visible. Calculations suggest that the low-energy peak is caused by a transition to the S_1 state of n−π* character; whereas the main absorption peak below 190 nm is caused by the strong transition to the S_2 state of mainly π−π* character.

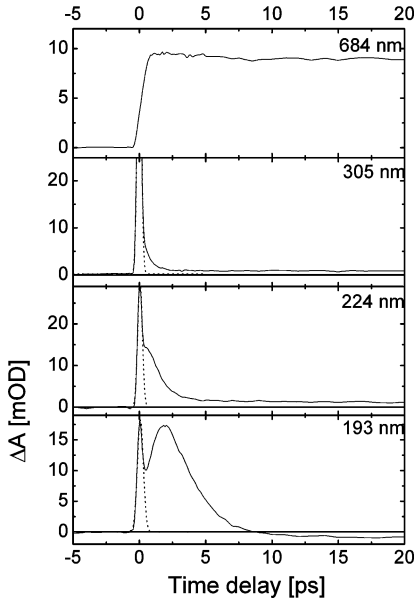

Figure 2. Representative time scans showing the induced absorption and bleaching following photolysis of formamide at 200 nm. The strong peak at $t = 0$ corresponds to the two-photon absorption of liquid water. At 193 nm the induced absorption is caused by vibrationally excited formamide. The weak negative absorption, visible after 10 ps is due to formamide molecules converted into CHO + NH_2. As the probe wavelength is increased, the induced absorption caused by vibrational relaxation appears and decays faster, as evident from the data at 224 and 305 nm. The NH_2 signal is also visible as part of the signal at long delays at 305 nm. At 684 nm the signal is caused by hydrated electrons generated from two-photon ionization of the water solvent. As the electrons are generated by absorption of 2 photons at 200 nm, the ejection length is large, and no recombination is observed for the delay times probed here.

The Gaussian function, shown as the dotted gray line in the figure, has a temporal width, approximately corresponding to the cross-correlation time of the pump and probe pulses. The spike is then followed by an increasing induced absorption, reaching its maximum at 2 ps and decaying to a negative (induced transparency) value in 7 ps. The decay follows a single exponential with a decay time of 2.4 ps with an asymptotic value of −1 mOD. As the probe wavelength is gradually tuned toward longer wavelengths, the initial Gaussian spike remains whereas the induced absorption both appears and decays faster.

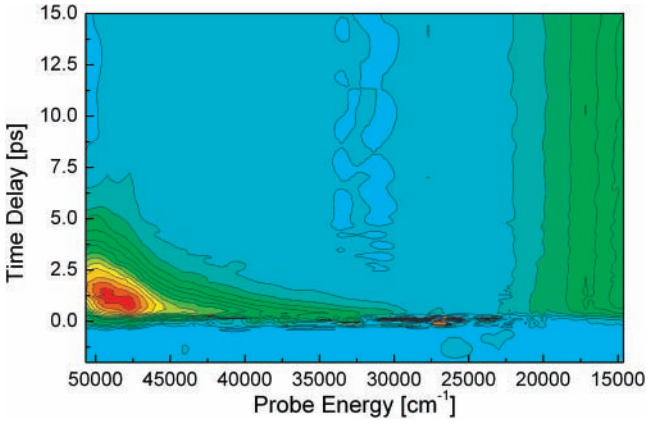

Figure 3. Vibrationally modulated formamide absorption. The maximum signal corresponds to a transient absorption of ~50 mOD, whereas the negative signal observed after 10 ps around 50 000 cm^{-1} corresponds to an absorption of −3 mOD. The spike at $t = 0$, corresponding to the (pump + probe) two-photon absorption in water was removed for clarity.

At 224 nm the absorption following the spike peaks at 0.6 ps and decays exponentially with a time constant of 1.1 ps. At 305 nm, the absorption is only seen as an asymmetric tail on the initial spike and the exponential decay time of the tail is 0.6 ps. Both at 224 and 305 nm we observe an induced absorption of a few mOD at long delays. Above 330 nm, only the spike remains and gradually a new component of the transient absorption becomes visible. This transient absorption rises in 1 ps and remains constant in the 20 ps window shown here. The amplitude of this component increases gradually as the probe wavelength is tuned further toward longer wavelengths. The spike amplitude reaches a maximum between 260 and 370 nm, and then decreases at longer wavelengths. The upper trace in Figure 2 shows the transient absorption at the 684 nm probe wavelength. The transient absorption seen in the long wavelength part of the spectrum as well as the short spike at shorter probe wavelength are well-known features representing the transient absorption spectrum of the solvated electron[21] and the two-photon (one pump and one probe photon) absorption of liquid water.[22] The induced absorption and transparency at short probe wavelengths bear the clear spectral signature of a vibrationally relaxing absorber,[23,24] where the decay time of the induced absorption becomes shorter as the probe wavelength is displaced from the center of the absorption band of the vibrationally excited molecule, in the present case formamide. In addition to the vibrational relaxation, the small induced transparency at 193 nm and the similar induced absorption at 224 and 305 nm observed after 10 ps is a clear indication of a photolytic conversion of formamide molecules into photo products, stable on the timescales investigated here. In Figure 3 we show a contour plot of transient absorption in the range from 193 to 684 nm, corresponding to 52 000 to 14 600 cm^{-1}, showing both regions: the region from where vibrational relaxation is most prominent and the onset of the absorption by the hydrated electron. From this figure it is again seen that as the probe wavelength is tuned to the low-energy side of the formamide absorption spectrum, the induced absorption decays faster and faster until only the initial spike remains, approximately at 30 000 cm^{-1}. Both Figures 2 and 3 show a very small induced transparency at the shortest probe wavelength and longest delays, indicating that formamide is the transient species responsible for the observed vibrational relaxation. This will be discussed further later in the paper.

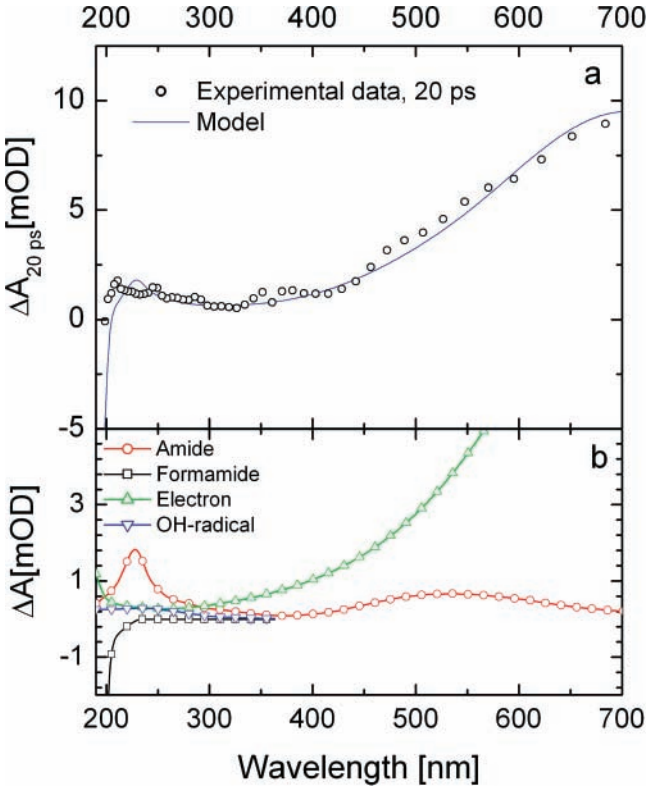

Figure 4. Experimental spectrum measured after 20 ps, where the transient spectral evolution has decayed (open circles). The full blue line is the calculated spectrum assuming dissociation of formamide into CHO and NH_2 and a small contribution from two-photon ionization of the water solvent. The model shown in a is based on the steady-state spectra and shown in b of OH[22,33,34] (blue triangles), NH_2[35,36] (red circles), e^-[21,37,38] (green triangles), and formamide (black squares), shown here scaled in proportion to their contributions to the spectrum shown in a.

For selected probe wavelengths we followed the time evolution of the transient absorption to 100 ps. The experimental data shows very little, if any, spectral developments after approximately 10 ps. In other words, all the processes responsible for the primary photochemistry of formamide are completed within 10 ps.

In addition to the measurements of spectral and temporal dynamics a number of additional measurements were performed to investigate the pump power dependence of the transient measured spectra. The induced absorption measured at 207 nm was observed to be linear in the power of the pump pulse. Furthermore, the induced absorption above 300 nm was also measured as a function of pump power, and a superlinear power dependence of the pump pulse was observed ($\sim I^{1.3}$). Both observations indicate a dominant contribution to the induced absorption below 300 nm from simple one-photon absorption in formamide and a small contribution from hydrated electrons and OH radicals, following two-photon ionization and dissociation of the water solvent.[22,25] In the following we will discuss the primary photoproducts observed and discuss the vibrational relaxation observed in terms of a simple 1-dimensional model for vibrational relaxation in aqueous formamide.

Discussion

From the transient spectrum observed after 20 ps, where the relaxation processes are completed, we are able to precisely deduce the primary photochemical reaction of formamide. Figure 4a shows a slice through the experimental data, obtained at 20

ps, showing the "steady-state" transient absorption following the 200 nm photolysis pulse at $t = 0$. Superimposed on the experimental data is a model spectrum based on the known steady-state absorption spectra, shown in Figure 4b, of the possible photoproducts. Most of these spectra are available in the literature, and references are given in Figure 4. Note, however that the spectrum of the formyl radical in aqueous solution is not known. As evident from Figure 4a, we are able to reproduce the experimental data by assuming that formamide dissociates into the formyl radical (CHO) and the amide radical (NH_2)

$$HCONH_2 \xrightarrow{\hbar\omega} HCO + NH_2 \quad (1)$$

From the amplitude of the transient spectrum at 20 ps we obtain a concentration of ~10 mM of the NH_2 reaction product, in good agreement with a simple estimate based on the available pump energy and the extinction coefficient and concentration of $HCONH_2$.

Although the initial bleaching of the formamide transition is difficult to extract precisely, we estimate that 10 mM only constitutes a small fraction of the total number of excited formamide at $t = 0$. Approximately 80% of the formamide molecules excited at $t = 0$ returns to the ground state of formamide (vibrationally excited) within the time resolution of our experiment (~300 fs), and of the remaining 20% roughly one-half the molecules recombine diffusively on a time scale of approximately 25 ps, whereas the other half remains separated during the time window investigated in this work. As in our previous studies of the photolysis of formic acid and the formate ion,[13,14] we see no spectral indication of the formyl radical.

To account for the experimental observations, we also include a small contribution from two-photon ionization and dissociation of liquid water.[22,25]

$$H_2O \xrightarrow{2\hbar\omega} H_3O^+ + OH + e_{aq}^- \quad (2)$$

$$H_2O \xrightarrow{2\hbar\omega} H + OH \quad (3)$$

Even though the yield is very small, ~3 mM of water molecules are excited, the contribution becomes visible as a result of the large extinction coefficients of both the hydrated electron and the OH radical. We note that the signal caused by the hydrated electron above 500 nm, where no other photoproducts contribute significantly, is nearly constant in time. This is in good agreement with the notion that the electron is formed predominantly through two-photon excitation of water. Thereby, the electron gains substantial kinetic energy and, as a consequence, localizes far from the parent water molecule, preventing recombination on a subnanosecond time scale.[26] The spectra shown in Figure 4b have all been scaled in accordance with the concentration estimates given above to show their contributions to the model spectrum shown in Figure 4a together with the experimental data.

As noted above, the transient spectral signature observed from 0 to 10 ps is a clear indication of vibrational relaxation of hot $HCONH_2$. As a starting point, we will consider the recombination/relaxation process as a simple one-dimensional process involving only the C−N stretch coordinate in formamide. Dissociation of formamide to CHO + NH_2 will obviously involve stretching of the C−N bond, and consequently, we model the dissociation/recombination process as a geometric distortion of the formamide molecule along the one molecular

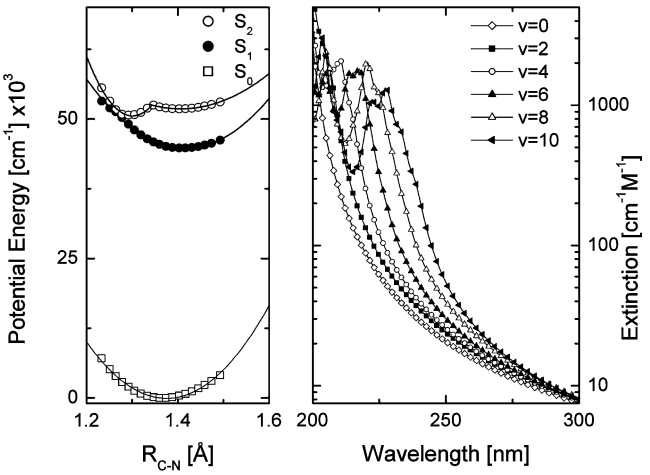

Figure 5. (a) Potential-energy curves for the ground state and first two excited states of formamide along the C−N stretch coordinate. For clarity, the curves are depicted as a function of the C−N distance relevant for dissociation of formamide. (b) Corresponding electronic absorption spectra of vibrationally excited formamide in $\upsilon = 0$, 2, 4, 6, 8, 10.

normal mode vibration that most closely resembles a C−N stretch at 1262 cm^{-1}.

We envision the process as an initial excitation to a potential-energy surface of formamide, which is unstable along the C−N stretch coordinate. Then, either during the first encounter with the surrounding water molecules, or as a result of a fast internal conversion process, or both combined, energy is exchanged and the formamide molecule is left in the electronic ground state. Most of the binding energy will then reside in the C−N stretch coordinate, which will then relax to the vibrational ground state within a few picoseconds. This is likely to be an oversimplification as several low-frequency modes of formamide could be active in the relaxation process, thereby facilitating the coupling to the solvent. Nevertheless this *single-mode* relaxation model has previously been able to account for the recombination/relaxation observed in ClO_2 and CS_2 under similar conditions.[23,27] Furthermore, as will be shown below, the very fast dissipation of vibrational energy to the solvent within 2 ps suggests that very little time is available to channel the C−N bond vibrational energy into other formamide modes through IVR.

The first 10 ps of the transient absorption spectrum below 35 000 cm^{-1}, depicted in Figure 3, is consequently interpreted as being dominated by the ground-state absorption spectrum modulated by the excited C−N stretch vibration. A simple estimate of the absorption spectrum of vibrationally excited formamide can thus be calculated from a one-dimensional wavepacket model[28,29] once the potential-energy surfaces of the relevant states have been calculated.

In Figure 5a we show the calculated potential energy obtained from an electron structure calculations of the ground and the two lowest excited singlet states in formamide. For clarity, we have shown the potential energy as a function of the C−N distance, but the calculation was performed for the true asymmetric stretch coordinate. The level of calculation is the CIS(D)/aug-cc-pvdz method using a ground-state geometry obtained at the B3LYP/G-311+G(d,p) level. The curvature of the potential energy reproduces the vibrational frequency near 1268 cm^{-1} observed for the C−N stretch of gas-phase formamide in the electronic ground state. Optical transitions are allowed to both the S_1 and S_2 states, but the oscillator strength to the S_2 state is much stronger than that to S_1. The absorption

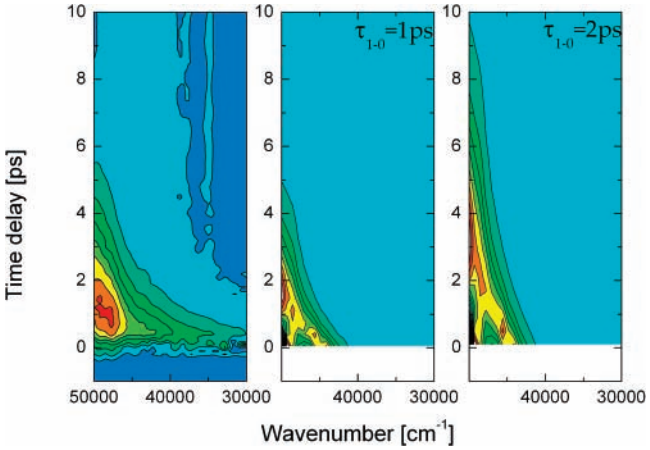

Figure 6. Comparison between the experimental data and two simulations of the vibrationally modulated formamide spectrum. The simulated spectra correspond to a vibrational energy relaxation time of the $v = 1$ of $\tau_{01} = 2$ ps or $\tau_{01} = 1$ ps.

spectra of formamide, shown in Figure 1, is composed of contributions from the weak transition to the S_1 state of n−π* character peaking at 220 nm and the strong transition, peaking at ~180 nm, to the S_2 state of $\pi-\pi$* character. We assume that the excitation at 200 nm primarily populates the S_2 state with a minor contribution from the S_1 states.

From the potential-energy curves in Figure 5a we can calculate the absorption spectrum of formamide for excited C−N vibrations.[30] The absorption spectra are shown in Figure 5b for even vibrational levels up to $v = 10$. We used a logarithmic scale to emphasize the absorption on the low-energy side of the line center, which increases with increasing v. To compare these spectra with the experimental data shown in Figure 3, we adopt a simple model where the rate of vibrational energy relaxation is proportional to the vibrational quantum number v,[31] and the vibrational energy is initially localized in the $v = 10$ level. In the present case, we thus use the vibrational relaxation time from $v = 1$ to 0, τ_{10} as the adjustable parameter, and scale the relaxation from higher vibrational levels according to their energy. Assuming a lifetime of the $v = 1$ state of either 2 or 1 ps, we obtain the spectra of relaxing formamide shown in Figure 6 together with the observed spectra. First, we note that there is a qualitative agreement between the calculated and observed spectra, which we take as verification of the assumption that vibrational relaxation is the main cause for the observed spectral evolution during the first 10 ps. Second, it is also evident that the simple simulation is not able to capture the details of the vibrational relaxation process in formamide. We believe that three factors influence the agreement between experiment and simulation in the present case. First, we must extend the range of ground-state vibrational levels used in the calculation. Initially, most of the binding energy resides in the C−N stretch coordinate, and the present calculation including $v = 10$ only accounts for roughly 25% of this energy. Second, we must investigate the interplay between vibrational energy transfer to the solvent and internal redistribution of the vibrational energy. We would expect that a highly excited C−N stretch vibration could couple to the low-frequency modes in formamide, leading to a fast redistribution of the vibrational energy within the formamide molecule. However, the very strong coupling to the water solvent, we observe the dissipation of 4−6 eV in a few picoseconds, indicates that only very strong intramolecular interactions will be able to compete with the direct dissipation of the energy of the C−N stretch vibration to the surrounding water molecules. This efficient channeling of the vibrational energy away from the molecule could also prove to be a key element in the photostability of certain biological molecules. To be photostable, the molecule must have a fast solvent-assisted pathway from the excited electronic states to the ground state as well as a strong coupling to the acceptor modes in the solvent. The density of low-frequency (<1000 cm^{-1}) acceptor modes in liquid water is very high due to the intermolecular hydrogen bonds and, furthermore, the formamide molecule is effectively coupled to these modes through hydrogen bonding.[20,32] Both the carbonyl oxygen and the amide hydrogen form a H bond with water with a bond strength of the order of 20−30 kJ/mol.

Finally, close inspection of the potential-energy curves in Figure 5a reveals near crossing of the S_1 and S_2 curves, suggesting the presence of a conical intersection. Consequently, a more detailed investigation of the excited-state potential curves could provide a much more detailed picture of the competition between internal conversion and photodissociation in formamide. Presently, it is not possible from the experimental data to decide if the excited formamide molecules follow the same potential-energy surface to dissociation, whereafter some molecules cage back and reform ground-state formamide, or if the hot formamide ground state is formed in an internal conversion process different from the path leading to dissociation of the molecule.

Conclusions

We studied the photolysis of aqueous formamide using femtosecond pulses at 200 nm. The appearance of the photoproducts was monitored with time-resolved absorption spectroscopy in the range from 193 to 700 nm. The majority of the excited formamide molecules return to the ground state within the first picosecond after excitation. Subsequently, we observe a strong red shift of the ground-state absorption spectra of formamide due to vibrational excitation. Vibrationally excited formamide rapidly dissipates the vibrational energy to the solvent, and the spectrum blue shifts toward the ground-state absorption spectrum. After 10 ps the relaxation is complete. A smaller fraction of the excited formamide molecules dissociate to CHO + NH_2, of which 50% escape recombination on the time scale investigated here. In agreement with previous work, we see no spectral signature of the formyl radical. The vibrationally modulated absorption spectrum of formamide constitutes a precise probe on the detailed processes taking place, when vibrational energy is dissipated in an aqueous environment. We performed a simple theoretical investigation of the process using time-dependent wavepacket propagation on the first and second excited state of formamide. Although simplistic in its approach, the simulation provides a qualitative confirmation of the observed spectral modulation of the formamide absorption spectrum.

Acknowledgment. This work was supported by the Danish Natural Science Research Council, Grant No. 272-06-0570, and the Danish Center for Scientific Computing, HDW-0107-13-(AU).

References and Notes

(1) Hare, P. M.; Crespo-Hernandez, C. E.; Kohler, B. *Proc. Natl. Acad. Sci. U.S.A.* **2007**, *104* (2), 435−440.

(2) Satzger, H.; Townsend, D.; Zgierski, M. Z.; Patchkovskii, S.; Ullrich, S.; Stolow, A. *Proc. Natl. Acad. Sci. U.S.A.* **2006**, *103* (27), 10196−10201.

(3) Pecourt, J. M. L.; Peon, J.; Kohler, B. *J. Am. Chem. Soc.* **2001**, *123* (42), 10370−10378.

(4) Basch, H.; Robin, M. B.; Kuebler, N. A. *J. Chem. Phys.* **1968**, *49* (11), 5007.

(5) Besley, N. A.; Oakley, M. T.; Cowan, A. J.; Hirst, J. D. *J. Am. Chem. Soc.* **2004**, *126* (41), 13502−13511.
(6) Coyle, J. D. *Chem. Rev.* **1978**, *78* (2), 97−123.
(7) Hill, R. R.; Coyle, J. D.; Birch, D.; Dawe, E.; Jeffs, G. E.; Randall, D.; Stec, I.; Stevenson, T. M. *J. Am. Chem. Soc.* **1991**, *113* (5), 1805−1817.
(8) Volman, D. H. *J. Am. Chem. Soc.* **1941**, *63* (7), 2000−2002.
(9) Hayon, E.; Nakashima, M. *J. Phys. Chem.* **1971**, *75* (13), 1910−1914.
(10) Liu, D.; Fang, W. H.; Fu, X. Y. *Chem. Phys. Lett.* **2000**, *318* (4−5), 291−297.
(11) Park, J.; Ha, J. H.; Hochstrasser, R. M. *J. Chem. Phys.* **2004**, *121* (15), 7281−7292.
(12) Lundell, J.; Krajewska, M.; Rasanen, M. *J. Phys. Chem. A* **1998**, *102* (33), 6643−6650.
(13) Thogersen, J.; Jensen, S. K.; Christiansen, O.; Keiding, S. R. *J. Phys. Chem. A* **2004**, *108* (37), 7483−7489.
(14) Petersen, C.; Thogersen, J.; Jensen, S. K.; Keiding, S. R. *J. Phys. Chem. A* **2006**, *110* (10), 3383−3387.
(15) Unpublished results.
(16) Rocha, W. R.; Martins, V. M.; Coutinho, K.; Canuto, S. *Theor. Chem. Acc.* **2002**, *108* (1), 31−37.
(17) Schuchmann, M. N.; Von Sonntag, C. *J. Am. Chem. Soc.* **1988**, *110* (17), 5698−5701.
(18) Sham, Y. Y.; Joens, J. A. *Spectrochim. Acta, Part A: Mol. Biomol. Spectrosc.* **1995**, *51* (2), 247−251.
(19) Madsen, D.; Larsen, J.; Jensen, S. K.; Keiding, S. R.; Thogersen, J. *J. Am. Chem. Soc.* **2003**, *125* (50), 15571−15576.
(20) Chang, Y. J.; Castner, E. W. *J. Chem. Phys.* **1993**, *99* (1), 113−125.
(21) Jou, F. Y.; Freeman, G. R. *J. Phys. Chem.* **1979**, *83* (18), 2383−2387.
(22) Thomsen, C. L.; Madsen, D.; Keiding, S. R.; Thogersen, J.; Christiansen, O. *J. Chem. Phys.* **1999**, *110* (7), 3453−3462.
(23) Poulsen, J. A.; Thomsen, C. L.; Keiding, S. R.; Thogersen, J. *J. Chem. Phys.* **1998**, *108* (20), 8461−8471.
(24) Walhout, P. K.; Silva, C.; Barbara, P. F. *J. Phys. Chem.* **1996**, *100* (13), 5188−5199.
(25) Elles, C. G.; Shkrob, I. A.; Crowell, R. A.; Bradforth, S. E. *J. Chem. Phys.* **2007**, *126* (16).
(26) Lian, R.; Oulianov, D. A.; Shkrob, I. A.; Crowell, R. A. *Chem. Phys. Lett.* **2004**, *398* (1−3), 102−106.
(27) Thomsen, C. L.; Thogersen, J.; Keiding, S. R. *J. Chem. Phys.* **2001**, *114* (9), 4099−4106.
(28) Kulander, K. C.; Heller, E. J. *J. Chem. Phys.* **1978**, *69* 2439.
(29) Poulsen, J.; Nymand, T. M.; Keiding, S. R. *Chem. Phys. Lett.* **2001**, *343* (5−6), 581−587.
(30) Kulander, K. C.; Heller, E. J. *J. Chem. Phys.* **1978**, *69* 2439.
(31) Oxtoby, D. W. *Annu. Rev. Phys. Chem.* **1981**, *32* 77−101.
(32) Dixon, D. A.; Dobbs, K. D.; Valentini, J. J. *J. Phys. Chem.* **1994**, *98* (51), 13435−13439.
(33) Pagsberg, P.; Christen, H.; Rabani, J.; Nilsson, G.; Fenger, J.; Nielsen, S. O. *J. Phys. Chem.* **1969**, *73* (4), 1029.
(34) Madsen, D.; Thomsen, C. L.; Thogersen, J.; Keiding, S. R. *J. Chem. Phys.* **2000**, *113* (3), 1126−1134.
(35) Buxton, G. V.; Lynch, D. A. *J. Chem. Soc., Faraday Trans.* **1998**, *94* (21), 3271−3274.
(36) Pagsberg, P. AEK-Risø 256; 1972.
(37) Nielsen, S. O.; Michael, B. D.; Hart, E. J. *J. Phys. Chem.* **1976**, *80* (22), 2482−2488.
(38) Nielsen, S. O.; Pagsberg, P.; Hart, E. J.; Christen, H.; Nilsson, G. *J. Phys. Chem.* **1969**, *73* (9), 3171−&.